Chapter 2

Basic Theory of NMR Imaging

Introduction

NMR imaging is a 3-D imaging system that uses the NMR phenomenon as an imaging tool. Magnetic resonance is a phenomenon found in magnetic systems that posses both magnetic moment and angular momentum. In this case, the term *resonance* means that we are in tune with the frequency of gyroscopic precession of the magnetic moment of nuclei in an external static magnetic field. In NMR imaging, we select a region from samples and obtain spatial distributions of nuclear spins through the application of spatial field gradients and RF signals. Thus, the cross-sectional images of an object are obtained.

The advantages of NMR imaging are its nonhazardous nature, its high-resolution capability, its capability of obtaining anatomical cross-sectional images in any direction, and its high tissue discrimination capability.

In the early 1970s, both Lauterbur and Damadian showed that NMR spectroscopic techniques could be applied to imaging the human body. In 1978, Andrew demonstrated the very high resolution capability of NMR by obtaining a detailed image of the septum of a small lemon. Moore and Holland soon followed with images of the human head, demonstrating the potential of NMR imaging in diagnostic imaging.

An interesting aspect of NMR imaging is its diversity in image formation. The formation of a NMR imaging system requires a magnet, gradient coils, RF coils, computer, and associated electronics. A main-field strength of 0.5 to 20 kG is used with a field gradient of 0.01 to 1 G/cm. The resolution in a conventional NMR imaging system depends on the field homogeneity and the strength of field gradients.

Basic Theory of NMR

All materials, whether organic or inorganic, contain nuclei, which are protons, neutrons, or a combination of both. Nuclei that contain an odd number of protons, neutrons, or both in combination posses a nuclear *spin* and a *magnetic moment*. This situation is equivalent to the bulk of many small magnets.

When a given material is placed in a magnetic field, the randomly oriented nuclei experience external magnetic torque, which tends to align the nuclei in both parallel and

antiparallel directions to the applied magnetic field. The spinning nucleus responds to the external magnetic field like a gyroscope precessing around the direction of the gravitational field. The rotating or precessional frequency of the spins, called the Larmor precession frequency, is proportional to the magnetic field strength.

When proton nuclei are placed in a magnetic field, the nuclei are in two energy states $+\mu H_0$ (antiparallel) and $-\mu H_0$ (parallel to the static magnetic field H_0, where μ and H_0 are the nuclear magnetic moment and applied magnetic field, respectively. At thermal equilibrium the distribution of spins in energy states follows the Boltzmann law, the lower energy state has a larger population of spins than the higher energy state. The irradiation of external electromagnetic radiation of energy E equivalent to $2\mu H_0$ tends to excite protons at the $-\mu H_0$ energy states up to the higher energy $+\mu H_0$ state. This energy is given in the form of RF magnetic field H_1. The excited protons then tend to return to their low-energy state, producing the free induction decay (FID) signal.

Two relaxation mechanisms are associated with these excited nuclear spins: transverse or spin-spin relaxation and longitudinal or spin-lattice relaxation. The imaging capabilities of two important parameters, spin-lattice relaxation (T_1) and spin-spin relaxation (T_2) together with the spin densities of the object, make NMR imaging a unique and powerful technique in diagnostic imaging.

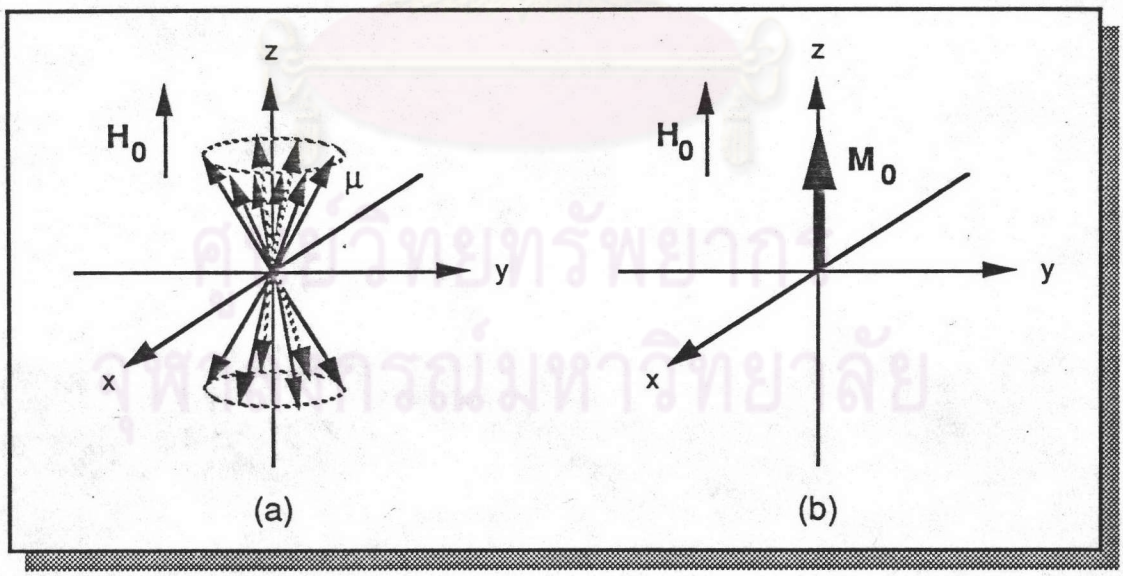

Fig. 2-1 Spins in a magnetic field H_0. (a) Spins precess in two energy states. (b) Net spin magnetization vector M_0.

Let us consider a magnetic moment μ in the presence of a magnetic field H_0. Fig. 2-1 (a) shows the precession of proton spins in two energy states. All moment precess about H_0 at

the same frequency, but without phase coherence in the x-y plane. Since the Boltzmann distribution, at equilibrium there are more nuclei aligned in the direction of H_0. The net magnetization vector M_0, which is the vector sum of μ's, is oriented along the z axis.

The precession of spin follows the Larmor precession frequency, which is unique to each nucleus.

$$\omega_0 = -\gamma H_0 \tag{1}$$

To considering the motion of the magnetization, we use a rotating frame of reference, a set of Cartesian coordinates (x', y', z') rotating about H_0 at an angular frequency ω. The magnetic field associated with this frame is called the effective magnetic field, which is given by

$$H_{eff} = H + \omega/\gamma \tag{2}$$

In the absence of an RF field, $H = H_0$. At resonance, the fictitious field ω/γ exactly cancels H, and H_{eff} becomes zero. When the static magnetic field is in the z direction and the RF field H_1 is applied along the x' direction (H_1 is rotating in the x-y plane), the total magnetic field H is

$$H = H_0 \hat{z} + H_1(\hat{x} \cos \omega t + \hat{y} \sin \omega t) \tag{3}$$

Inserting Eq. (3) into Eq. (2), H_{eff} becomes

$$H_{eff} = \left(H_0 - \frac{\omega}{\gamma}\right)\hat{z}' + H_1 \hat{x}' \tag{4}$$

At resonance ($\omega=\omega_0$), Eq. (4) can be expressed as $H_{eff} = H_1$. Thus, the only magnetic field is in the x' direction, and M precesses around the x' axis with frequency γH_1. For a time-varying RF field $H_1(t)$, the flipping angle is given by

$$\theta = \gamma \int_0^{t_p} H_1(t)\, dt \tag{5}$$

where t_p is the RF pulse duration. The flipping of magnetization M into the x-y plane is illustrated in Fig. 2-2.

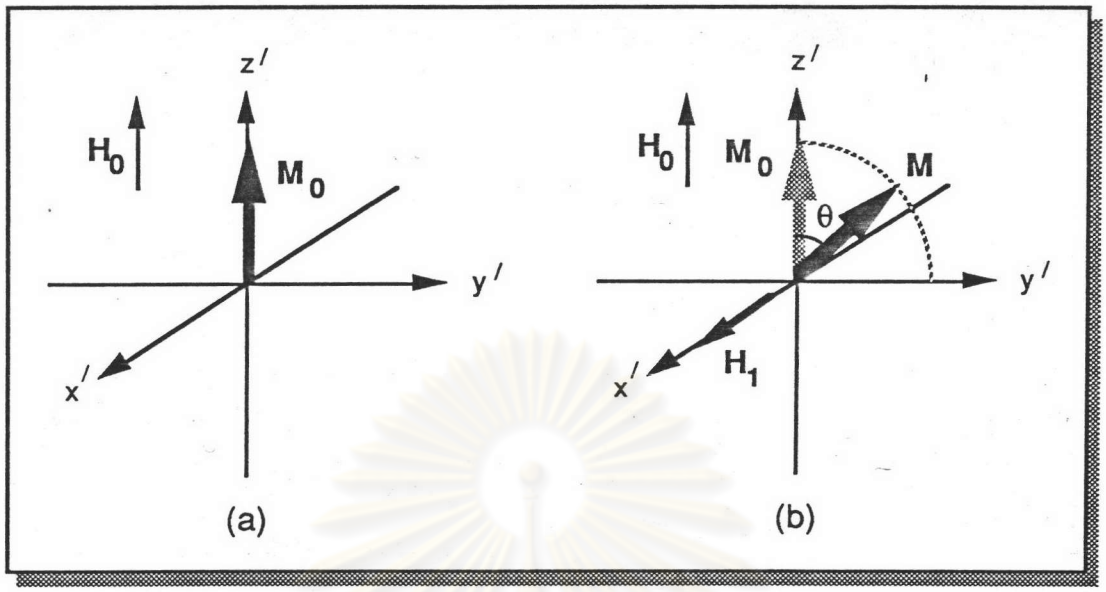

Fig. 2-2 Spin magnetization in the rotating frame. (a) Spin in the absence of RF pulse. (b) Spin flip with an application of the RF field H_1.

When H_1 is applied along the x' axis for a pulse period t_p, the spin flips through an angle θ from the z' axis toward the y' axis. In general, θ is set at $\pi/2$ or π, depending on the mode of excitation.

After H_1 is turned off, the rotating magnetization induces a current into the pickup coil surrounding the object. The magnetization then relaxes, through neighboring spins, to its thermal equilibrium, so that the spins realign with the H_0 field direction. On the other hand, the transverse component of magnetization, decays through the spin-spin interaction and dephases. This transverse (spin-spin) relaxation time is denoted by T_2.

In addition to the spin-spin relaxation, there are other dephasing effects, such as the magnetic field inhomogeneity and field gradients. In NMR imaging, magnetic field gradients are added to resolve the spatial distribution of spin density. In fact, they produce shifts in the Larmor frequencies throughout the sample, resulting in a phase incoherency that eventually makes the composite sinusoidal signal decay more rapidly. In other word, an effective transverse relaxation time T_2^* is smaller than T_2.

The composite sinusoidal signal decaying with the relaxation time T_2^*, as shown in Fig. 2-3, is then detected with a phase-sensitive detector. The results are similar to a decaying demodulated AM signal.

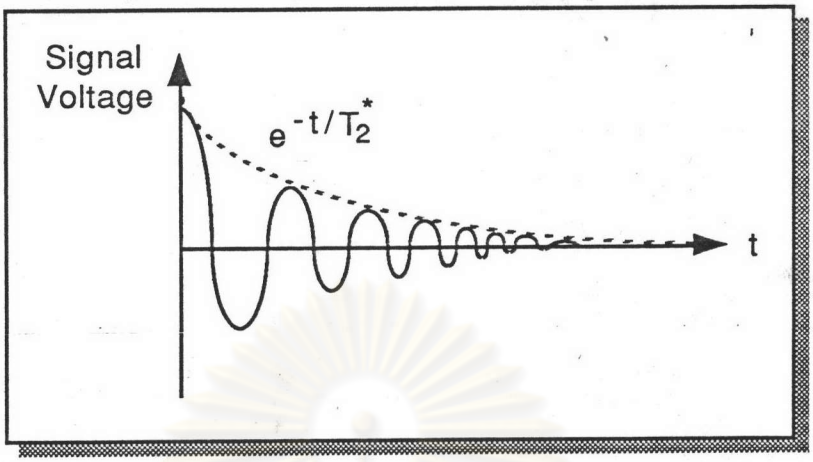

Fig. 2-3 FID signal obtained indicates a modulated decaying signal.

Concurrently, longitudinal or spin-lattice relaxation forces the spins to realign in the H_0 direction, because it is the thermal equilibrium state. Because it involves energy dissipation through the lattice, the longitudinal relaxation time T_1 is usually longer than T_2 and is related to the z component of magnetization, as shown in Fig. 2-4.

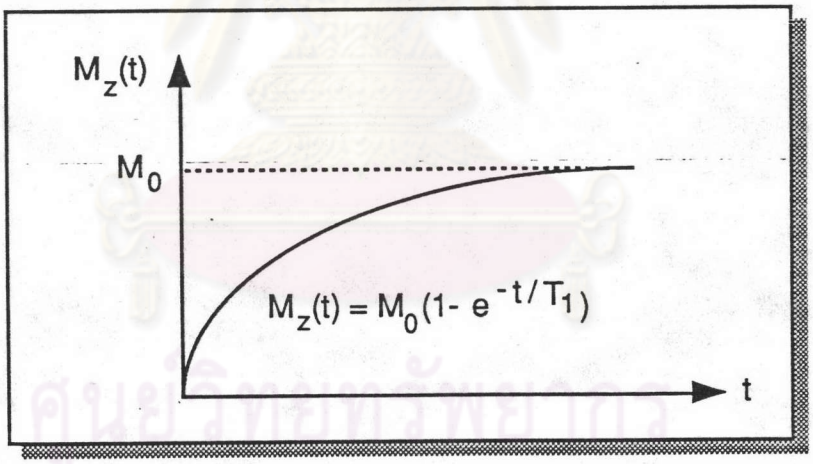

Fig. 2-4 Spins decay by spin-lattice relaxation mechanism.

The two relaxation processes work simultaneously and vary greatly depending on the characteristics of the material. In Fig. 2-5, sequential pictures of the relaxation processes are shown.

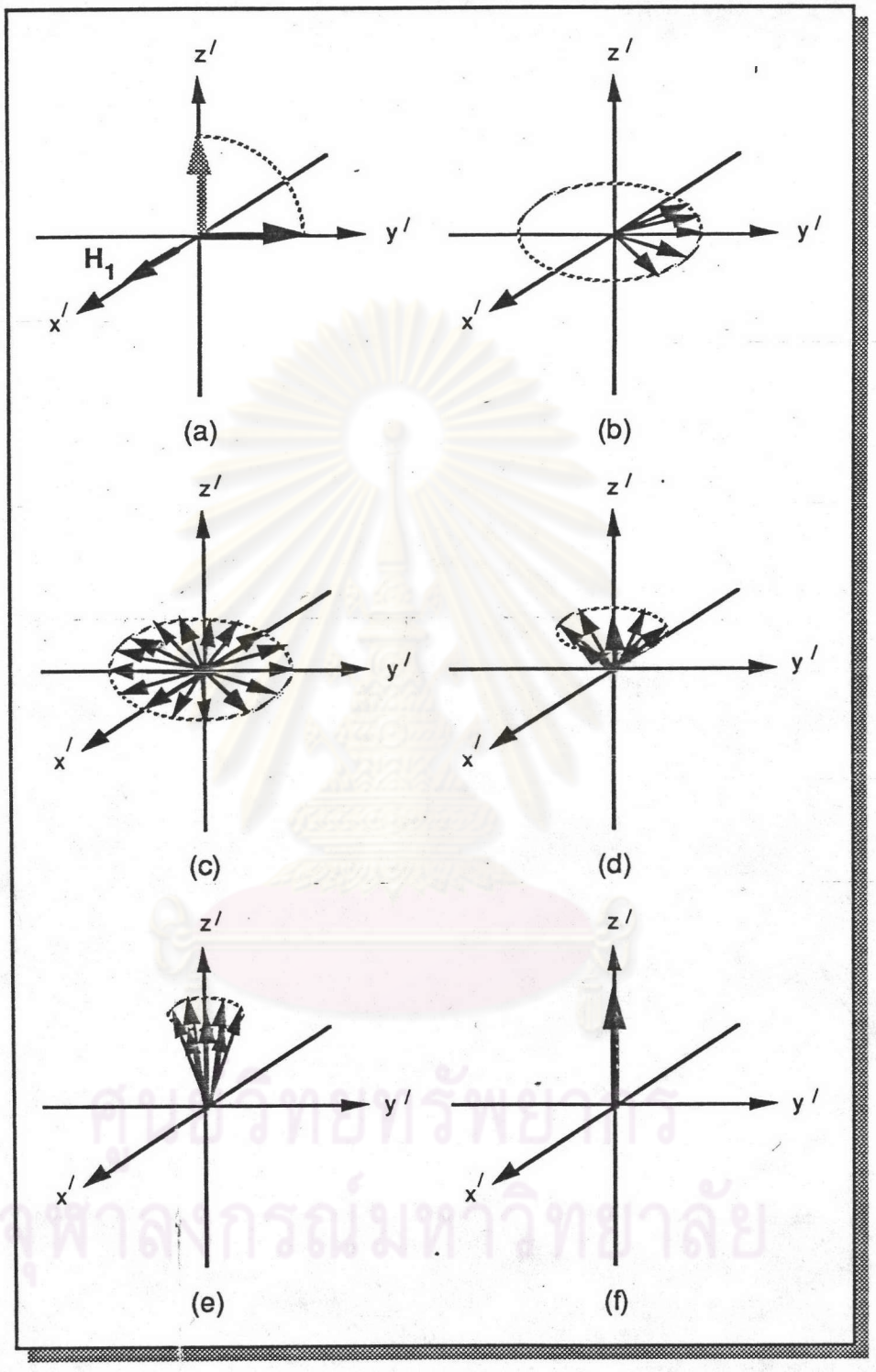

Fig. 2-5 Sequential illustrations of spin relaxation processes. (a) Spins are flipped by the RF pulse. (b) Spins are dephased due to spin-spin relaxation and field inhomogeneity. (c) FID signal decays to zero as the spins lose phase coherence. (d-f) spins relax to the original equilibrium state by the spin-lattice relaxation process.

Several forms of spin-echo techniques play an essential role in data acquisition for NMR imaging. The two basic forms are the Hahn spin-echo technique and the Carr-Purcell Meiboom-Gill (CPMG) technique. In the Hahn spin-echo technique (Fig. 2-6), a 90° RF pulse is applied to the direction of the x' axis, and then the magnetization vector **M** rotates to the y' axis. The spin magnetizations then dephase over time, due to field inhomogeneity or added field gradients. A subsequent 180° pulse applied along the x' axis rotates the spins around the x' axis. The spin magnetizations now continue to precess but begin to rephase. At this point, all the spins are completely rephased along the -y' axis, but the magnetizations have now decayed by T_2 relaxation.

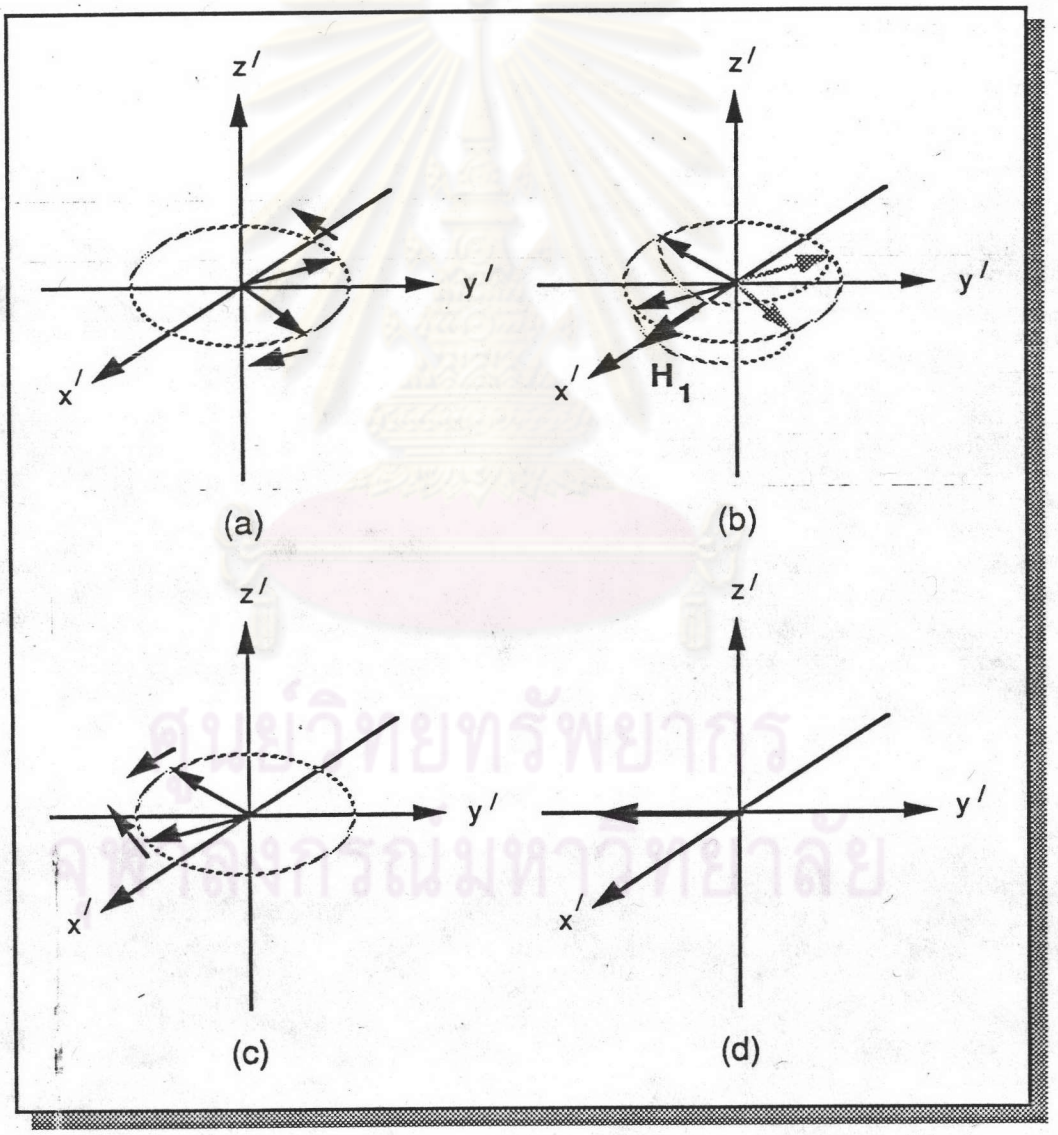

Fig. 2-6 Hahn spin echo. (a) Spin magnetization dephase after 90° rotating by RF pulse. (b) 180° pulse is applied along x' axis. (c) The spins are being refocused. (d) Spin echo is generated along -y' axis.

In the CPMG method (Fig. 2-7), a 180° pulse is applied along the y' axis instead of the x' axis, so that the spin flips around the y' axis.

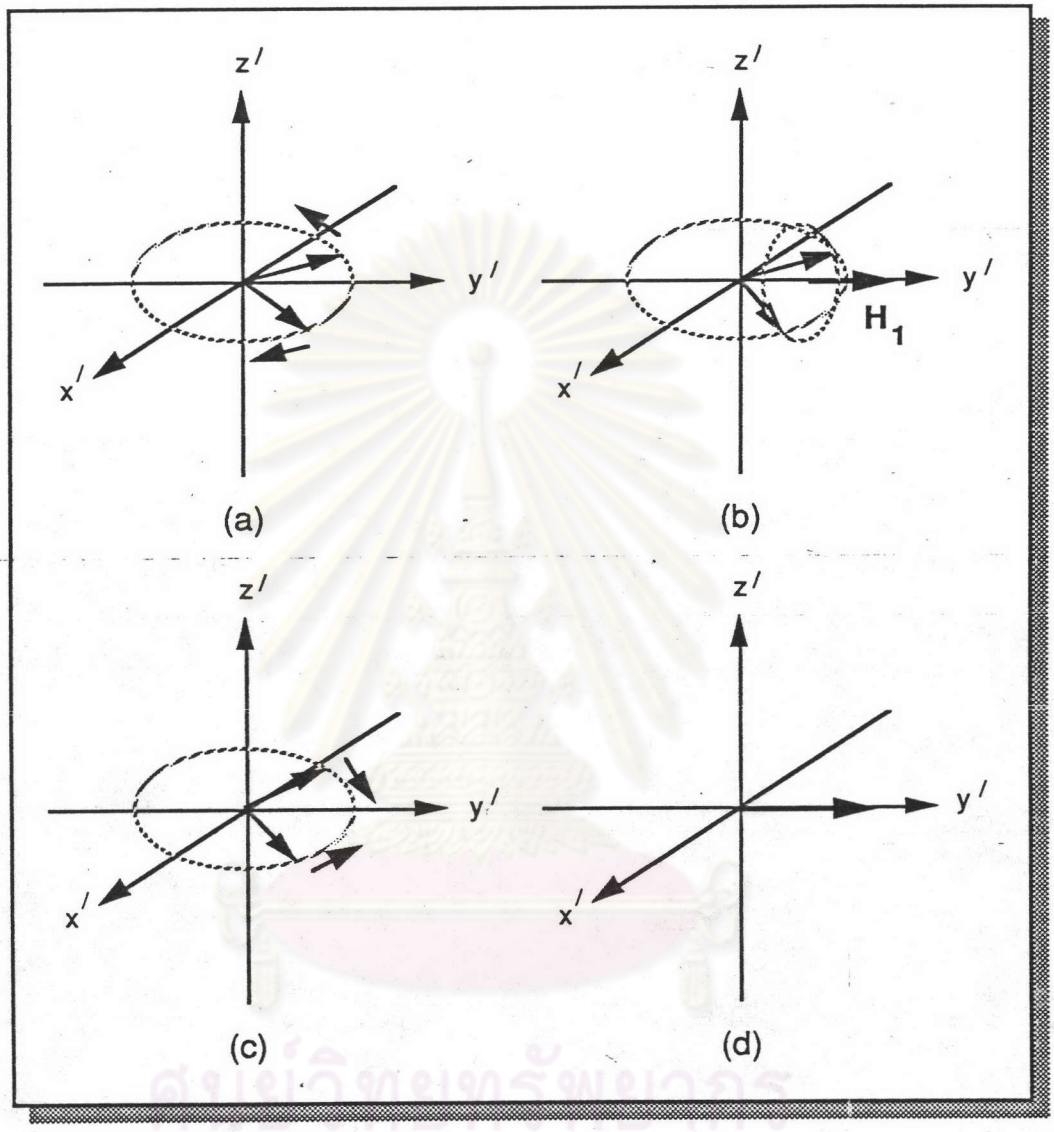

Fig. 2-7 CPMG spin echo. (a) Spin magnetization dephase after 90° rotating by RF pulse. (b) 180° pulse is applied along y' axis. (c) The spins are being refocused. (d) Spin echo is generated along y' axis.

Basic Theory of NMR Imaging.

Conventional NMR spectroscopy requires an extreme homogeneity magnetic field to reduce the frequency shift effect caused by the spatially dependent field variations. In NMR imaging, a field gradient is deliberately added to resolve the spatial distribution of spins into Fourier domain components. The basic form of signal obtained from 3-D Fourier transform NMR, which is known as FID, is expressed as

$$s(t) = M_0 \int_{-\infty}^{\infty} \int_{-\infty}^{\infty} \int_{-\infty}^{\infty} f(x,y,z) \exp\left\{ i\gamma \int_0^t \left[xG_x(t') + yG_y(t') + zG_z(t') \right] dt' \right\} dx\, dy\, dz \qquad (6)$$

where f(x,y,z) is the 3-D spin density distribution and $G_x(t)$, $G_y(t)$, and $G_z(t)$ are the time dependent field gradients along the x, y, and z axis, respectively. The generated FID is, in effect, a Fourier transform-domain representation of the spin density distribution.

Direct Fourier Imaging

One of the interesting aspects of NMR imaging is that the NMR images can be formed by many different procedures. In NMR imaging, data acquisition pulse sequences play an important role and are related to the image reconstruction algorithms employed. The method of projection reconstruction is the earliest technique by which NMR images acquired relied on reconstruction from a given set of projections of the sample. Nowadays, direct Fourier imaging technique, which has the advantage on simplicity in reconstruction, is in common use as far as general clinical applications are concerned.

This direct Fourier imaging (DFI) method was first proposed by Kumar, Welti, and Ernst. In this case, imaging can proceed through the total 3-D excitation of an object in series of time sequences.

In this procedure, three orthogonal field gradients, G_x, G_y, and G_z are applied in sequence after 90° RF excitation pulse at t=0. The z component of the local magnetic fields are then given as

$$H_z(x,y,t) = \begin{cases} H_0 + G_z z, & \text{for } o < t < t_z \\ H_0 + G_y y, & \text{for } t_z < t < t_z + t_y \\ H_0 + G_x x, & \text{for } t_z + t_y < t < t_z + t_y + t_x \end{cases} \qquad (7)$$

The FID signal is sampled when the x gradient is applied. The sampled FID signal reflects the previous application of the z and y gradients by retaining the phase change caused by those gradients. For this reason, this imaging scheme is often called the phase-encoding method. The series of FID signals obtained with the various t_z and t_y then form a full 3-D FID signal set sufficient for reconstruction of the spin density image of the entire volume.

The observed FID signal $s(t_x,t_y,t_z)$ is expressed as

$$s(t_x,t_y,t_z) = M_0 \int_{-\infty}^{\infty} \int_{-\infty}^{\infty} \int_{-\infty}^{\infty} f(x,y,z) \exp\left[i\gamma\left(G_x x t_x + G_y y t_y + G_z z t_z\right)\right] dz\, dy\, dx \tag{8}$$

Fourier transform of Eq. (8) results in spatial spin density function as

$$\tilde{f}(\omega_x,\omega_y,\omega_z) = \int_{-\infty}^{\infty} \int_{-\infty}^{\infty} \int_{-\infty}^{\infty} s(t) \exp\left[-i\left(\omega_x t_x + \omega_y t_y + \omega_z t_z\right)\right] dt_z\, dt_y\, dt_x \tag{9}$$

The reconstructed image is then related to f(x,y,z) as

$$\tilde{f}(\omega_x,\omega_y,\omega_z) = k f\left(\gamma x G_x, \gamma y G_y, \gamma z G_z\right) \tag{10}$$

where k is a constant.

Fig. 2-8 shows RF and gradient pulse sequences of conventional DFI using spin echo for one-slice 2-D imaging. In this scheme, although the whole volume of an object is excited by the 90° RF pulse, only the spins in a designated slice are rephased to form an echo through the application of a narrow-band 180° RF pulse and z directional selection gradient. Note that the x directional phase encoding is achieved by varying the amplitude of the x gradient instead of varying the time interval.

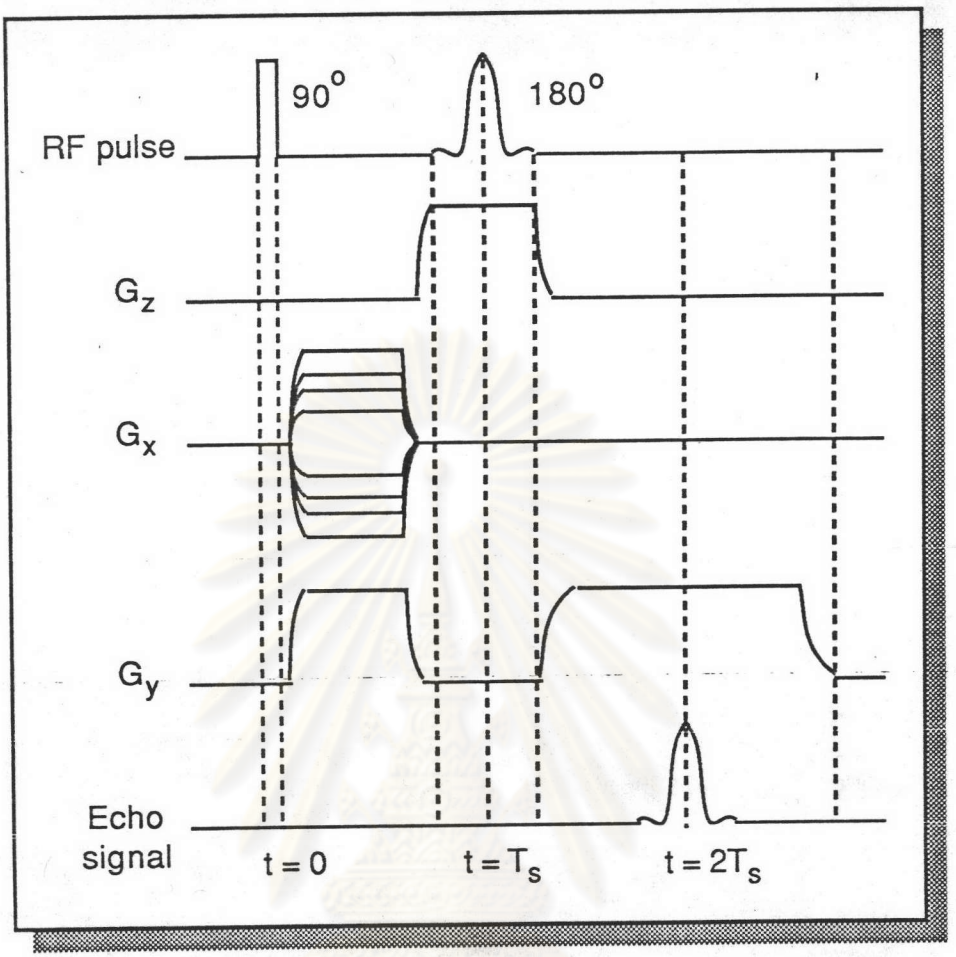

Fig. 2-8 Imaging sequences of 2-D direct Fourier imaging. The slice in the z direction is selected and spin echo is used.

Imaging Modes

The spin density f(x,y,z) obtained by the imaging methods described above is not a real spin density; it is weighted by T_1 or T_2 or both. Because T_1 or T_2 varies between normal and abnormal tissues, the image of spin density weighted by T_1 or T_2 has been found to be clinically useful. However, several attempts have been made to extract T_1 information, as well as spin density and T_2. The typical imaging modes currently in use are described.

1. Saturation Recovery Imaging

The saturation recovery method involves simply repeating the pulse sequence at regular intervals T. The equations discussed previously are unchanged except for the replacement of f(x,y,z) with f'(x,y,z), which is expressed as

$$f'(x,y,z) = f(x,y,z)\left\{1 - \exp\left[-T / T_1(x,y,z)\right]\right\} \qquad (11)$$

2. Inversion Recovery Imaging

Inversion recovery is similar to saturation recovery, except that the 180° RF pulse precedes the 90° RF pulse with a time interval of T_1.

$$f'(x,y,z) = f(x,y,z)\left\{1 - 2\exp\left[-T_1 / T_1(x,y,z)\right]\right\} \qquad (12)$$

This technique is often used for measuring T_1 values in tissues.

3. Spin-Echo Imaging

Through the application of the 180° pulse following the first 90° pulse at $t = T_s$, spins are refocused at $t = 2T_s$ by the spin echo (Fig. 2-8). Although the spins are now refocused and coherent, the amplitude of FID decays exponentially with time constant T_2. The decayed spin density can be written as

$$f'(x,y,z) = f(x,y,z)\exp\left[-2T_s / T_2(x,y,z)\right] \qquad (13)$$

As explained above, the image is now weighted by T_2 as well as by T_1. By setting the appropriate T_s values, images weighted mainly by T_2 can be obtained, provided that the repetition time is sufficiently large.

Parameter Imaging Methods

The capability of extracting many functional parameters is one of the most important advantages of NMR imaging. Flow velocity, T_1, T_2, and chemical shift are some of the interesting parameters in NMR imaging that are discussed in this section.

1. Spin-Lattice Relaxation Time and Spin-Spin Relaxation Time

The effects of T_1 and T_2 are closely related to the NMR imaging modes. In T_1 imaging, both the saturation recovery and inversion recovery modes can be used. By varying the recovery time and observing the resulting image intensity variation, one can deduce T_1 values. Similarly, by changing the echo time ($2T_s$) in Eq. (13) for the spin-echo method, one can obtain several images differently weighted by T_2. From the images obtained with different echo times., T_2 values of each pixel can be calculated.

2. Flow Imaging

In NMR imaging, one can also measure the flow of nuclear spins through observation of the FID signal. In the first attempt at flow velocity measurement, two RF coils were used: one for the excitation of spins and the other for reception. If the maximum signal is received at Δt

seconds after the excitation with the distance Δl between two RF coils, the velocity can be estimated by $\Delta l/\Delta t$.

3. Chemical-Shift Imaging

Before NMR imaging was proposed, NMR had been used primarily for chemical spectroscopy, in which the frequency spectrum of a specific kind of nuclei was obtained. The chemical shift was usually measured for homogeneous samples under the condition of uniform field.

In spectroscopic NMR imaging, however, the chemical spectrum for each pixel is to be measured neither for the homogeneous samples nor under the uniform field condition but with spatially varying gradient pulses.